P-type β-Gallium Oxide: A new Perspective for Power and Optoelectronic Devices

Ekaterine Chikoidze[a]*, Adel Fellous[a], Amador Perez-Tomas [b], Guillaume Sauthier [b], Tamar Tchelidze[c], Cuong Ton-That[d], Tung Thanh Huynh[d], Matthew Phillips[d], Stephen Russell[e], Mike Jennings[e], Bruno Berini[a], Francois Jomard [a], Yves Dumont [a]

[a]Groupe d'Etude de la Matière Condensée (GEMaC), Université de Versailles Saint Quentin en Y. – CNRS, Université Paris-Saclay, 45 Av. des Etats-Unis, 78035 Versailles Cedex, France

[b]Catalan Institute of Nanoscience and Nanotechnology (ICN2), CSIC and The Barcelona Institute of Science and Technology, Barcelona, Spain

[c]Faculty of Exact and Natural Science, Department of Physics, Ivane Javakhishvili Tbilisi State University, 3 Av. Tchavtchavadze, 0179 Tbilisi, Georgia

[d]School of Mathematical and Physical Science, University of Technology Sydney, Broadway, PO Box 123, NSW 2007, Australia

[e]Faculty of Science, University of Warwick, Coventry CV4 7AL, U.K

corresponding author: E-mail : ekaterine.chikoidze@uvsq.fr

Abstract:

Wide-bandgap semiconductors (WBG) are expected to be applied to solid-state lighting and power devices, supporting a future energy-saving society. Here we present evidence of *p*-type conduction in the undoped WBG β-Ga_2O_3. Hole conduction, established by Hall and Seebeck measurements, is consistent with findings from photoemission and cathodoluminescence spectroscopies. The ionization energy of the acceptor level was measured to be 1.1eV above the valence band edge. The gallium vacancy was identified as a possible acceptor candidate based on thermodynamic equilibrium Ga_2O_3 (crystal) – O_2 (gas) system calculations (Kroger theory) which revealed a window without oxygen vacancy compensation. The possibility of fabricating large diameter wafers of β-Ga_2O_3 of p and n type nature, provides new avenues for high power and deep UV-optoelectronic devices.

Key words: Wide band gap semiconductor, beta-Ga_2O_3, electrical properties, hole conductivity, thermodynamic calculations

1. Introduction

Ga_2O_3 has recently attracted considerable interest for its unique combination of material properties [1,2] and relevance to many present and future application fields: extreme (also referred

to as so-called "ultra") wide bandgap semiconductors (≥ 4.8 eV) for deep-ultraviolet optoelectronics, very large breakdown electrical field ($E_{br} = 8\times10^6$ V cm^{-1}) for high voltage and power electronics. Indeed recent breakthroughs in material quality have led to a "rediscovery" of β-Ga_2O_3 as an ultra-wide bandgap transparent conductor [3]. Demonstrators include transparent field-effect transistors [4], photodetectors [5,6], use as a material for microwave and optical maser [7], as well as a material for electroluminescent devices [8] and chemical sensing [9]. Moreover, its very wide bandgap and large disruptive critical electrical field has allowed Ga_2O_3 to emerge as the fourth generation material platform for power electronics [10,11], (after silicon, silicon carbide and gallium nitride) [12,13].

Nevertheless, all the Ga_2O_3 devices demonstrated thus far are unipolar (only *n*-type) [2,14-18]. In order to realize the full potential for WBG (opto)electronics β-Ga_2O_3, will need bipolar junction based devices, for which p-type doping will be required. The bipolar junction would be engineered by combining *p*-type transparent TCOs with either, *n*-type Ga_2O_3 or the common *n*-type ones (namely In_2O_3, SnO_2 and ZnO and its alloys) into transparent *p*–*n* heterojunctions in a range of thin-film transistor applications. *P*-type requirement is also important in the power electronics context, where a high current carrying capability is desirable when considering applications such as grid-level converters. *P*-type Ga_2O_3 would allow the definition of Ga_2O_3 *p*-*n* junction building blocks and therefore any traditional Silicon-type devices would be engineered; including metal-oxide-semiconductor transistor field-effect devices (MOSFETs), (complementary) CMOS logic or bipolar devices such as pin diodes or insulator gate bipolar transistors (IGBT).

The current approach to achieve hole conductivity in Ga_2O_3 devices is by the definition of heterostructures of known *p*-type semiconductors such as *p*-type oxides (Ir_2O_3 [19], NiO_x [20]) or acceptor doped semiconductors (Si [21], SiC [22,23] or graphene [5]), with known disadvantages of crystalline and electronic band structure miss-matches. P doping in Ga_2O_3 is hugely challenging as an oxide (oxide usually has tendency of formation donor type oxygen vacancies, causing n-type conduction) and as an ultra-wide bandgap material, intrinsic conductivity is rare and even doping ("*p*" and "*n*") is normally not symmetrical. This lack of hole conductivity is probably the main limitation of emerging gallium oxide technology.

Currently, *p*-type wide bandgap oxides are in the form of binary copper oxides [24]. Cu-based delafosites [25], tin monoxide [26], nickel oxide [27] or layered oxide-chalcogenides [28]. Each of these have a valence band made of eep localized oxygen *2p* orbitals, which are responsible for poor hole transport in these materials [29]. Owing to its extreme wide bandgap, doping *p*-type *β*-Ga_2O_3 has been considered practically challenging-if not impossible. Usually nominal undoped as grown *β*-Ga_2O_3 single crystals and thin films are generally n-type, because of the existence of unintentional impurities [30, 31]. *P*-type conductivity was theoretically predicted in gallium oxide by doping group I and II metals from the Mendeleyev table [32,33].

However, there is no experimental demonstration of this in the literature up to date. Some of the challenges to be overcome in order to realize hole conductivity are [34]: /*i*/ very wide bandgap, /*ii*/ high formation energy of point defects that are *hole producers*, *e.g.* native acceptors such as cation vacancies, /*iii*/ small ionization energy for these defects so as to readily release holes, *i.e.*, a shallow acceptor level with respect to the host valence band; and most crucially /*iv*/ low energy of *hole killer* native defect donors such as cation interstitials and anion vacancies. In particular oxygen vacancies act as compensating donors and both as grown β-Ga_2O_3 films and bulk crystals are invariably found to be *n*-type in the literature [30,31].

This work reveals (via a range of characterization techniques) that intrinsic majority hole conduction can exist and emerge in nominally undoped β-Ga_2O_3, when compensation by background native donors is reduced.

2. Material and methods

Commercial pulsed laser deposition grown Ga_2O_3/*c*-sapphire epiwafers were provided by Nanovation (www.nanovation.com) [35]. The thickness of the gallium oxide films was around 300 nm, estimated using optical reflection interferometry with an Ocean Optics Nanocalc system. As a reference, *n*-type sample commercial Si-doped β-Ga_2O_3 from Novel Crystal Technology, Inc was used in case of photo-spectroscopy study. While for cathodoluminescence measurement we had commercial *n*-type β-Ga_2O_3 single crystal from MTI Inc. SEM images were recorded with a JEOL JSM 7001F electron microscope.

The crystallographic structure of the films was analyzed by X-ray diffraction (XRD) with a Siemens D-5000 diffractometer using Cu-K_α radiation (λ = 1.54 Å). Topography of the films had been investigated by AFM (Bruker Dimension 3100) in tapping mode using commercial tips with 300 kHz resonant frequency and 40 N m^{-1} spring constant. Secondary-ion mass spectrometry (SIMS) was carried out with the aid of a Cameca IMS 4f tool. X-ray photoelectron spectroscopy (XPS) and ultraviolet photoelectron spectroscopy (UPS) measurements were performed with a Phoibos 150 analyzer (SPECS GmbH, Berlin, Germany) in ultra-high vacuum conditions (basic pressure 3×10^{-10} mbar). XPS measurements were performed with a monochromatic K_α X-ray source (1486.74 eV). UPS measurements were realized with a monochromatic HeI UV source (21.2 eV).

Optical transmission spectra were measured in 200-2000 nm spectral range with a Perklin Elmer 9 spectrophotometer.

Ti/Au electrical contacts were deposited by RF-sputtering. Hall Effect measurements were performed in a Van der Pauw configuration in the temperature range of 80 K to 300 K and for magnetic fields perpendicular to the film plane varying from -1.6 T to 1.6 T, using a high impedance measurement set-up which was custom designed for measurement of high resistance diamond samples. Carrier type testing was also done using Seebeck effect measurements at 300 K-400 K with a home built set-up (also specially adapted for high impedance samples) based on a Keithley SCS-4200 measurement station and cascade Microtech Kelvin probes.

Cathodoluminescence microanalysis of the films was conducted in an FEI Quanta 200 Environmental SEM equipped with a diamond machined parabolic light collector and a Hamamatsu S7011-1007 CCD spectrometer.

The thermodynamic equilibrium in the Ga_2O_3 (crystal)–O_2 (gas) system was modeled by the Kroger method of quasi-chemical equations. In this method, the creation of dominant defects and charge carriers are written as chemical reactions. The corresponding mass action laws, together with the electro-neutrality condition and impurity mass balance equation, give a system of equations for the concentrations of the main charged species (acceptor and donor defects, electrons and holes) existing in the crystal.

3. Results and discussion

3.1.Structural, chemical analyses

Fig. 1a shows a photograph of a 2 inch diameter β-Ga_2O_3 wafer that has undergone Scanning Electron Microscopy (SEM) and Atomic Force Microscopy (AFM). This characterization showed that the film has a fine granular surface morphology composed of an irregular agglomeration of grains on a tens-of-nm scale. Root Mean Squared roughnesses (R_{RMS}) were in the region of 7 nm (mean of three 1 µm ×1 µm areas) which is similar to other reported values (varying between 3 and 8 nm) for β-Ga_2O_3 thin films [36, 37].

The X-ray diffraction (XRD) 2 theta scan for the β-Ga_2O_3 / c-Al_2O_3 epiwafer (Figure 1b) reveals three different diffraction peaks located at 2θ values of 18.73°, 38.22°, and 58.87°. The peaks are indexed as the $(\bar{2}01)$, $(\bar{4}02)$ and $(\bar{6}03)$ reflections of monoclinic β-Ga_2O_3 (**Fig. 1b**) indicating a layer with a strong $(\bar{2}01)$ preferred orientation, as reported elsewhere for β-Ga_2O_3 films grown on c-sapphire [15,16,39].

Secondary Ion Mass Spectroscopy (SIMS) compositional depth profiling was performed for Si, Sn, Ge, P, N, and Al. Measurement profiles shown in **Fig. 1c** demonstrate that Ga_2O_3-sapphire interface is very sharp and clear. There was an absence of all cited impurities, above the level of the SIMS detection limit (10^{14} cm^{-3}).

The optical transmission spectrum (**Fig. 1d**) reveals that the transparency of the Ga_2O_3-on-Al_2O_3 wafer is higher than 80 % for 280-700 nm wavelength range, as is could be expected for undoped Ga_2O_3 [36,39-41]. The optical band edge was estimated to be around 230 nm.

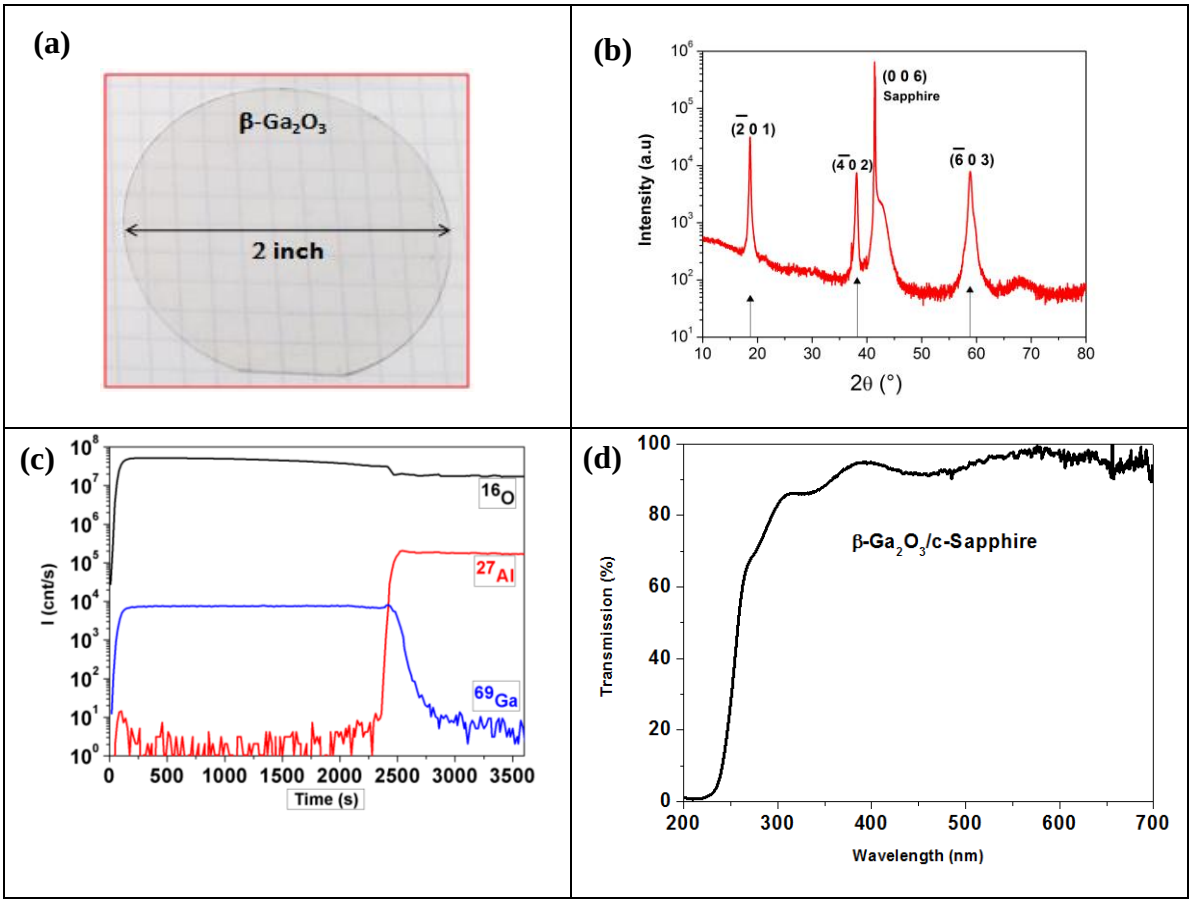

Fig. 1. (a) Photograph of a commercial, specially elaborated, 2-inch β-Ga_2O_3 / c-sapphire epiwafer from Nanovation; (b) Cu-K_α 2θ X-ray diffractogram, with arrows indicating β-Ga_2O_3 Bragg peak; (c) SIMS compositional depth profiles; (d) Optical transmission spectrum.

3.2. Electrical properties

Because of the WBG, nominally undoped β-Ga_2O_3 is generally highly resistive [2,42]. Deviations from oxygen stoichiometry (and in particular oxygen vacancies) have been invoked to explain a relatively high *n*-type conductivity observed in some nominally undoped Ga_2O_3 bulk crystals and thin films. However this hypothesis seems to be questionable as hybrid functional density calculations predict the oxygen vacancy to be a deep donor with ionization energy higher than 1 eV [29]. Higher n-type conductivity can also be efficiently achieved by impurity doping with Sn, Si, Ge, F or Cl [14]. A detailed study of the electrical transport properties of the *β*-Ga_2O_3 / *c*-Al_2O_3 structure was performed. Ohmic contacts were prepared by RF-sputtering of Ti (50 nm) / Au (200 nm) bilayers at the four corners of the sample (**Fig. 2b**).

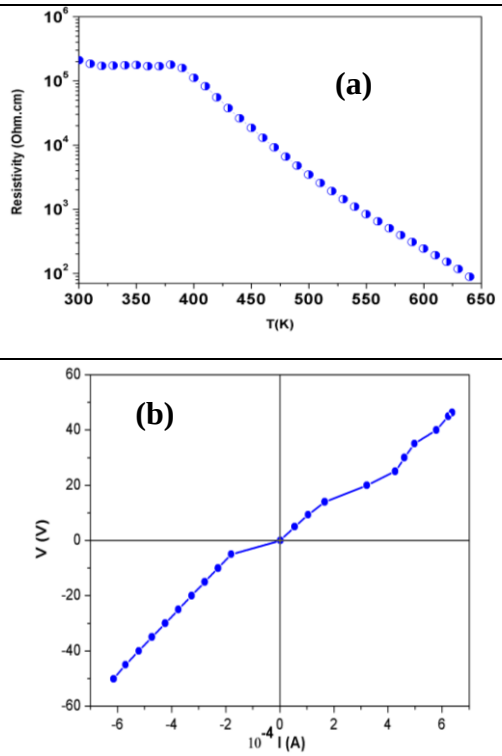

Fig. 2. (a) Resistivity versus temperature for β-Ga_2O_3 films on c-sapphire. (b) Voltage versus Intensity I-V characteristics.

The resistivity measured in a Van der Pauw configuration is as high as 2×10^5 Ω cm. Heating the sample up to 650 K leads, as usually happens for semi-insulating material, to a reduction of resistivity down to 1.8×10^2 Ω cm (**Fig. 2a**).

Van der Pauw Hall Effect measurements were employed to determine the carrier type, density and mobility. When the sample is of high resistance ($> 10^7$ Ω), determination of carrier type is not trivial, due to the difficulty in correctly extracting the Hall voltage (V_H) from the total

measured voltage. To validate the measurement, applied magnetic field dependence of V_H was performed at different temperatures. In non-magnetic material, V_H is linearly proportional to applied magnetic field and positive sign indicates that the majority charge carriers are p-type (holes). Hall voltage measurements at varying magnetic fields (0-1.6 T) and several temperatures (520-610 K), highlight positive V_H, which linearly increase with perpendicularly applied magnetic field. This implies that the epilayer is *p*-type (**Fig. 3**).

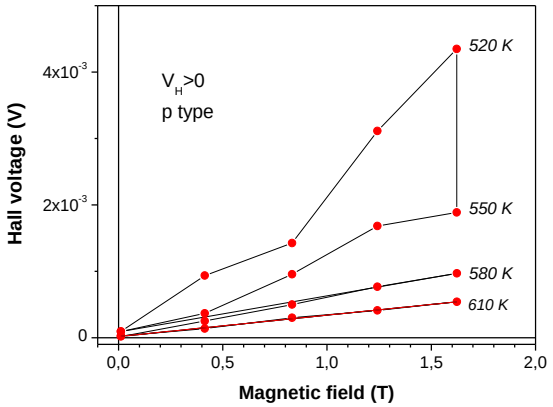

Fig. 3 Hall voltage V_H versus applied perpendicular magnetic field at different temperatures.

The carrier type was confirmed using a home-built Seebeck effect measurement setup, specially adapted for high resistive samples. Measurements were performed with the same sample, utilizing the Ti/Au Ohmic contacts. A Seebeck coefficient with a positive sign was obtained, confirming the majority carriers to be holes. The Seebeck coefficient, *S*, was +36 μV K^{-1} at room temperature.

The temperature dependence of the hole concentration, p (cm^{-3}), is shown in (**Fig. 4a)**. These characteristics exhibit a hopping conductivity regime in the 300-400 K range, and a band activated regime in the 400-650 K temperature range. This is characteristic of (a) deep acceptor level(s). A further study of the acceptor ionization energy E_i (eV) has been made.

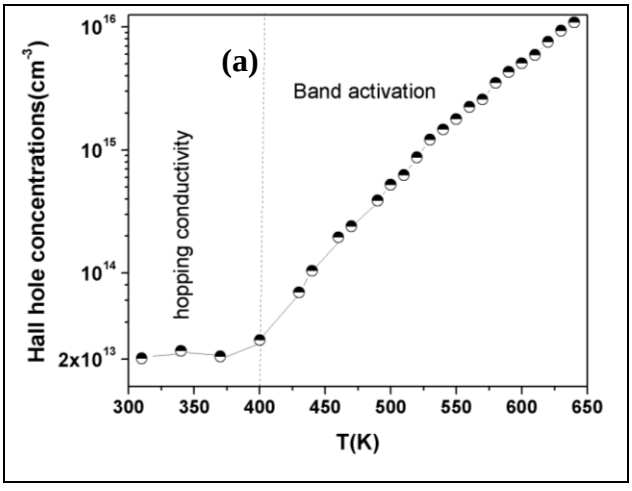

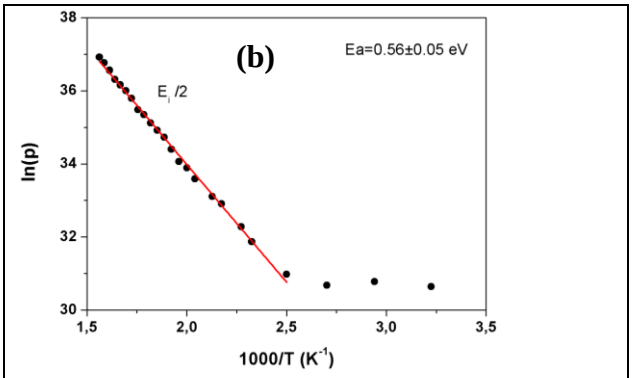

Fig. 4 (a) temperature dependence of the hole concentration p. (b) *ln(p)* versus *1000/T* plot leading to a carrier activation energy

$E_a = 0.56 \pm 0.05$ eV.

For a *p*-type semiconductor, the general description of the hole concentration at a temperature *T* (K) is given by the neutrality equation:

$$\frac{g_d\, p(N_D + p)}{M_v(N_A - N_D - p)} = \exp\left(-\frac{E_i}{kT}\right) \qquad (1)$$

Where *k* is Boltzmann's constant (m^2 kg s^{-2} K^{-1}), g_D is the acceptor degeneracy, and N_A is the acceptor concentration (cm^{-3}), N_D is the compensating donor concentration (cm^{-3}), M_V is the hole density of states in the valence band.

At higher temperatures, (in the region where experimental measurements were carried out) in the so-called negligible compensation regime where $N_A >> p >> N_D$, the activation energy is $E_i/2$, and p is given by:

$$p = \left[\frac{N_A M_v}{g_d}\right]^{\frac{1}{2}} \exp\left(-\frac{E_i}{2kT}\right) \qquad (2)$$

The carrier activation energy, E_a, is obtained from a linear regression in a *ln(p)* versus *1000/T* plot (**Fig. 4b**). A value of $E_a = 0.56 \pm 0.05$ eV was found. In this low compensation regime, the relationship between defect activation and ionization energies is $E_i = 2E_a$, meaning that the ionization energy of the acceptor defect responsible for the conductivity is around $E_i = 1.12$ eV. Hall mobility of holes does not change significantly within the 300-650 K temperature interval, increasing from 0.2 cm^2 V^{-1} s^{-1} at 300K (in the hopping regime) to 4.2 cm^2 V^{-1} s^{-1} at 650 K (in the band activation regime). In *n*-type, β-Ga_2O_3 thin films, Hall mobility is typically relatively low (below 30 cm^2 $V^{-1}s^{-1}$), as in other WBG oxide semiconductors [43 - 45]. The significantly lower hole mobility measured in these p-type films could be explained by the large effective mass value of holes estimated by Varley *et al*. [46]. We have studied also much thinner, 70 nm β-Ga_2O_3 sample. It shows similar conductivity, carrier activation energies and *p*-type majority carriers.

3.3. Evidences of Acceptor Levels

3.3.1. Cathodoluminescence

Cathodoluminescence was performed at 80 K for our p-type epilayer and, by comparison, for an *n*-type β-Ga_2O_3 commercial single crystal from MTI Inc. (**Fig. 5**).

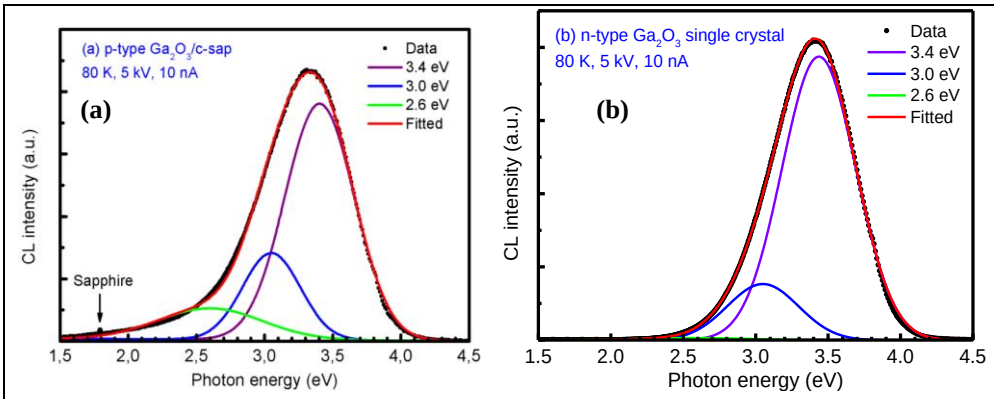

Figure. 5. CL spectrum for (a) the *p*-type β-Ga_2O_3 film grown on the *c*-plane sapphire substrate and (b) *n*-type β-Ga_2O_3 single crystal with $(\bar{2}01)$ orientation hydrothermally grown by MTI Inc.

Based on literature reports on β-Ga_2O_3 luminescence [47-49], the spectra can be fitted with three components (**Fig. 5**a): a 3.4 eV ultraviolet (UV) peak shown in violet (with Full Width at Half Maximum (FWHM) = 0.60 eV), a 3.0 eV blue (BL) peak shown in blue (FWHM = 0.5 eV) and a green (GL) peak 2.6 eV shown in green (FWHM = 0.9 eV). The UV emission has been assigned to the recombination of an electron with a self-trapped hole (STH). The BL and GL have been attributed to native point defects, a donor V_O and either an acceptor V_{Ga} or a V_O-V_{Ga} complex, respectively. The GL is absent in the *n*-type crystal (**Fig. 5**b) but present in the *p*-type epilayer suggesting it could be a signature emission of the acceptors.

3.3.2. X-ray photoelectron and photoemission spectroscopy

The room temperature photoemission spectrum for the Ga*2p*, Ga*3p*, O*1s* and C*1s* core levels is shown in (**Fig. 6a**). The binding energy value of the core level for the Ga*2p* states at 1119.3 eV (as determined by M. Marcel *et al.* [50]) on cleaved β-Ga_2O_3 single crystals was used for calibrating the binding energy positions of the XPS spectra. The Ga2*p* states show a reasonably sharp structure with a FWHM of 1.8 eV. The main O*1s* level appears at 532.05 eV, while the photoelectrons from the filled Ga$3d^{10}$ give a peak at 21.3 eV (which is as expected based on reference studies [50]).

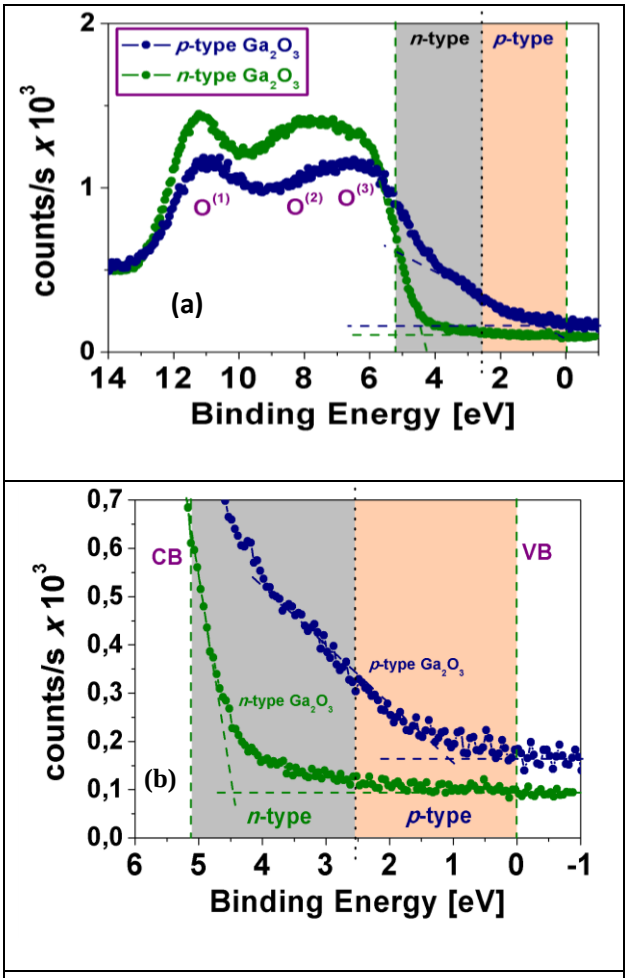

Fig. 6 (a) Valence band photoemission spectra for the reference Si-doped β-Ga_2O_3/β-Ga_2O_3 (*n*-type) and β-Ga_2O_3/*c*-sapphire (*p*-type). (b) zoom of the β-Ga_2O_3 band gap region.

The XPS spectra from the surface of a control sample of a 500 nm thick commercial (Novel Crystal Technology, Inc.) epiwafer of nominally *n*-type Si-doped β-Ga_2O_3 (N_d - N_a = 1.3×10^{18} cm^{-3}) grown on a single crystal β-Ga_2O_3 were used as a benchmark for the β-Ga_2O_3/*c*-sapphire valence band determination. The XPS spectrum has once again been calibrated with respect to the Ga2*p* energy at 1119.3 eV. The energies of O1*s* and Ga3*d* have been determined to be 522.07 eV and 21.4 eV, respectively. The binding energies of the core levels of the β-Ga_2O_3/*c*-sapphire and the control samples are, again, very similar.

There are however visible differences in the shape of the O1*s* level between the control (that exhibits a secondary shoulder at ~533 eV [51]) and the β-Ga_2O_3/*c*-sapphire surface, which has a more asymmetric peak centred at 532.05 eV. The O1*s* secondary shoulder is attributed to carbon surface contamination (in the form of C-O bonds) [50,51]. Another notable difference is the O2*s* peak (at a binding energy of ~ 25 eV) [57-59] which is clearly visible for the reference but is not observed for the β-Ga_2O_3/*c*-sapphire. The Ga3*d* reference peak is asymmetrical with a shoulder appearing at smaller binding energies (~ 20 eV). This shoulder was ascribed to the hybridization of Ga3*d* and O2*s* states near the valence band [51].

There also are remarkable differences between C1s core-level from the β-Ga_2O_3/*c*-sapphire and the Si-doped β-Ga_2O_3 homo-epitaxial reference. The relative amount of carbon at the surface is larger in the reference while the peak distribution is clearly different. While the reference C1s core level agrees well with a combination of C-O and C-H bonds, the β-Ga_2O_3/*c*-sapphire carbon signal seems to be primarily due to Ga-C bonds [45].

The covalent bonding interaction is due to the symmetry of the Ga*4s* states which enables a more energetically favorable bonding with the *p*-states of the oxygen. Several theoretical [54-56] and experimental studies [50-52,56] suggest that the partial density of states for the valence band is predominantly of O*2p* character while the conduction band states are predominantly derived from Ga*4s* and Ga*4p* states mixed with some contributions of O*2p*.

Very relevant for this study is the position of the Fermi level from the valence band, which is shown in **Fig. 6a**. From the valence band photoemission spectra it is possible to evaluate the electronic surface properties of the thin-films. The three maxima of the O*2p* valence band correspond to the three different oxygen sites in β-Ga_2O_3 ($O^{(1)}$, $O^{(2)}$ and $O^{(3)}$). The valence band width for the reference sample is around 8 eV, which is in agreement with previous reports [50]. Nevertheless, there is an exceptionally large number of tail states extending deeper in the bandgap for the β-Ga_2O_3 / c-sapphire surface compared to the reference n-type sample. The extrapolation of the first slope (at ~5×10^2 counts/s) gives Fermi level values of around 1.0 eV and 4.4 eV for the β-Ga_2O_3 / c-sapphire and control, respectively. It is also of note that there is a small but non-negligible number of states extending even deeper into the bandgap, with energies as low as ~ 0.5 eV above the valence band. These very remarkable differences in thin film valence band profiles are consistent with there being *p*-type conductivity in the β-Ga_2O_3/ *c*-sapphire epiwafer.

3.4. Thermodynamic analyses of point defect and charge carrier concentration equilibrium in Ga_2O_3

The thermodynamic equilibrium in the Ga_2O_3 (crystal) – O_2 (gas) system was modeled in order to define the dependence of point defects, charge carriers on temperature and oxygen partial pressure in the surrounding atmosphere. Knowing these dependences, the treatment temperature and oxygen pressure, for which creation of compensating donor defects are suppressed and acceptors and holes become dominant species can be determined. The analysis was made using the Kroger method of quasi-chemical equations [57]. In this approach, the creation of dominant defects and charge carriers are written as chemical reactions. The corresponding mass action laws, together with the electro-neutrality condition and impurity mass balance equation, give a system of equations for the concentrations of the main charged species (acceptor and donor defects, electrons and holes) existing in the crystal. As stated above, the main candidates for shallow donor and acceptor defects in β-Ga_2O_3, are gallium and oxygen vacancies, respectively. However, the association of gallium and oxygen vacancies is also considered as shallow compensating defect for *n*-type doping [43]. Proceeding from this, the main processes considered for the corresponding mass action law are the following:

The creation of a Schottky defect pair: $O \rightarrow 2V_{Ga} + 3V_O, \qquad K_S = [V_{Ga}]^2 [V_O]^3$ (3)

where K_S is reaction constants (**Table** 1).

The incorporation of oxygen atoms in a crystal from the surrounding atmosphere, when copper and chromium vacancies (V_{Cu} and V_{Cr}, respectively) are created:

$$\frac{3}{2}O_2 \rightarrow 3O_0 + V_{Ga}, \qquad K_{V_{Ga}} = \frac{[V_{Ga}]^2}{P_{O_2}^{3/2}} \tag{4a}$$

$$\frac{3}{2}O_2 \rightarrow 3O_O + 2V_{Cr}, \qquad K_{V_{Cr}} = \frac{[V_{Cr}]^2}{P_{O_2}^{3/2}} \tag{4b}$$

The lattice thermal ionization:

$$O \rightarrow e + h, \qquad K_i = np \tag{5}$$

where e and *h* are electrons and holes, respectively, and *n* and *p* their concentrations

The ionization of the gallium vacancy

$$V_{Ga} \rightarrow V_{Ga}' + \mathrm{h}, \qquad K_a = \frac{\left[V_{Ga}'\right]p}{[V_{Ga}]} \tag{6}$$

where $V_{Ga}^{'}$ is denote positively single-charged gallium vacancy

The ionization of the oxygen vacancy

$$V_O \rightarrow V_O^{\bullet} + e, \qquad K_d = \frac{\left[V_O^{\bullet}\right]n}{[V_O]} \tag{7}$$

where $V_O^{\bullet}$ is denote negatively single-charged oxygen vacancy

The association of vacancies:

$$V_O + V_{Ga} \rightarrow (V_{Ga} - V_O) \qquad K_{Ass} = \frac{\left[(V_{Ga} - V_O)\right]}{[V_{Ga}][V_O]} \tag{8}$$

where K_{Ass} is reaction constant of associated defect creation

The ionization of associate

$$(V_{Ga} - V_O) \rightarrow (V_{Ga} - V_O)' + h \quad K_{Ass}^{i} = \frac{\left[(V_{Ga} - V_O)'\right]p}{\left[(V_{Ga} - V_O)\right]} \tag{9}$$

where K_{Ass}^{i} is reaction constant for ionized $(V_{Ga}\text{-}V_O)'$ defect creation.

Charge neutrality condition

$$\left[V_O^{\bullet}\right] + p = n + \left[V_{Ga}'\right] \tag{10}$$

The temperature of oxygen treatment was fixed as 500°C and calculated dependence of concentrations on oxygen partial pressure. The results of solving equations (3)-(9) are given in (**Fig. 7)**.

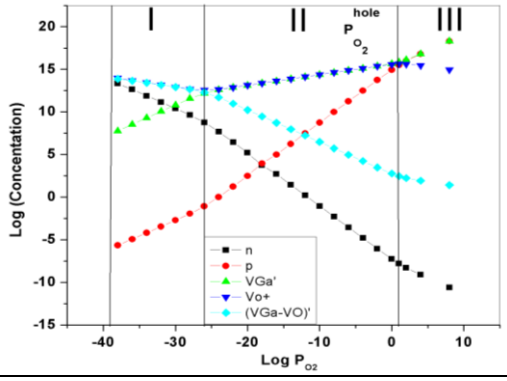

Fig. 7 Dependence of concentrations of charge carriers and charged point defects on oxygen partial pressure in Torr (= 1.33 mbar). $P_{hole} \approx 13.3$ mbar.

In figure the three regions are distinguished:

/i/ in the first region (left hand side) it is clearly seen that $\left[V_O^{\bullet}\right] = \left[\left(V_{Ga} - V_O\right)'\right]$ (11)

and these concentrations are the largest. Therefore eq. (8) can be simplified to (9) in this region.

/ii/ In the second region with increasing oxygen pressure, concentration of V_O decreases and compensation gets the form $\left[V_O^{\bullet}\right] = \left[V_{Ga}'\right]$ (12)

/iii/ in the third region, holes and acceptor vacancies are the dominant species and intrinsic hole conductivity should take place and $p = \left[V_{Ga}'\right]$ (13)

The pressures at which compensation type changes can be esasily found by means of discontinuity of the concentrations at the boundaries. For the boundary between the second and third region hole concentration on oxygen partial pressure is expressed as:

$$P_{hole} = \frac{K_s^{2/3} K_d^{2}}{K_g^{2} K_v^{2/3}} \quad (14)$$

P_{hole} is a very important quantity, because it can be considered as a measure of the strength of the compensation process. When the Fermi level lowers during *p*-doping, the creation enthalpy of intrinsic donor defects (vacancies) decreases, and high oxygen pressure is needed in the surrounding atmosphere in order to prevent evaporation of oxygen from the growing crystal. The higher the P_{hole}, the more difficult it is to achieve successful *p*-doping. **Fig. 7** shows, that for β-Ga_2O_3 at 500° C, $P_{hole} \approx 1.33\times10^{-2}$ atm with a hole concentration around $p \approx 10^{15}$ cm^{-3}. For comparison, calculations for ZnO give $P_{hole} \approx 10^{3}$ atm, for the same temperature [58]. The reason for such a difference might be most likely the higher formation energy of donor vacancies in β-Ga_2O_3 (approximatelly 1 eV higher per vacancy), making compensation mechanism by point defects less favorable in gallium oxide than in ZnO. Subsequently, it can be expected that *p*-type samples of β-Ga_2O_3 with higher carrier concentrations (then intrinsic) can be obtained when doping with shallow impurities.

Table 1. Reaction constants used in thermodynamic analyses.

Reaction	**Reaction constants**

$O \rightarrow 2V_{Ga} + 3V_O$	$K_S = 10^2 \exp(-18.4eV / k_B T)$ [59,60]
$3/2\,O_2 \rightarrow 3O_O + 2V_{Ga}$	$K_V = 10^2 \exp(-4.5eV / k_B T)$ *)
$O \rightarrow e + h$	$K_i = N_C N_V \exp(-4.8eV / k_B T)$ [61]
$V_{Ga} \rightarrow V_{Ga}' + \mathrm{h}$	$K_a = 2N_V \exp(-0.9eV / k_B T)$
$V_O \rightarrow V_O^{\bullet} + e$	$K_d = 2N_C \exp(-0.55eV / k_B T)$ [62]
$V_O + V_{Ga} \rightarrow (V_O - V_{Ga})$	$K_{ass} = \exp(2.25eV / k_B T)$ *)
$(V_O - V_{Ga}) \rightarrow (V_O - V_{Ga})' + h$	$K_{Ass}^{i} = 2N_c \exp(-0.42eV / k_B T)$ [47]

*) Estimated by means of approaches developed in F.A. Kroger, *"The chemistry of imperfect crystals"*, North-Holland Publishing Company, Amsterdam, 1964, pp.1039 [57]

Thus, Hall Effect, Seebeck, photoemission spectroscopy and cathodoluminescence spectroscopy studies, show that, nominally undoped β-Ga_2O_3 / *c*-sapphire epiwafers exhibit intrinsic majority *p*-type conduction. Acceptor candidate V_{Ga} or its complexes, are supported by the thermodynamic equilibrium of Ga_2O_3 (crystal)–O_2(gas) system calculations (Kroger theory), showing a "window" without oxygen vacancy V_O compensation (a common donor in transparent oxides). Hole conduction in the β-Ga_2O_3 semiconductor is possible. This situation is a crucial step towards the realization of effective *p*-type doping. This fact distinguishes β-Ga_2O_3 from other WBG oxides (ZnO, SnO_2 or In_2O_3), where *p*-type is similarly a challenge. Such a particularity is related with physical-chemistry of the point defects in Ga_2O_3, mainly that the enthalpy of creation of Schottky defects, is quite high (at approximately 3.68 eV per vacancy). Consequently, the creation of donor oxygen vacancies is not as favorable as in ZnO for example. This decreases the compensation possibility, making hole conduction favorable. Intrinsic low hole conductivity is achieved only in transparent oxides such as $CuCrO_2$ [63,64], Cu_2SrO_2 [65,66], NiO [67], and $FeTiO_3$ [68], each having much lower band gaps (~ 3.2 - 3.5 eV) than β-Ga_2O_3.

4. Conclusion

Attaining this relatively low level of *p*-type doping in gallium oxide may already be an important step for technological integration. Mainly, in power applications, the *p*-type conductivity is particularly important as the *p*-*n* junction could sustain larger voltages than any Schottky unipolar junction. The ultra-large critical field of Ga_2O_3 could only seriously be exploited in *p*-*i*-*n* structures [69]. In other words, the demonstration of Ga_2O_3 bipolarity represents a definitive step forward when taking into account this potentially low-cost oxide wide band gap semiconductor technology in power applications now dominated by the prohibitively expensive Silicon Carbide substrates.

In optoelectronics applications, the demonstration of p-type Ga_2O_3 is also relevant. A high performance, ultra-wide bandgap *p*-type transparent conducting oxide (TCO) would leverage the great promise of oxides for transparent electronics and optoelectronics. Owing to their ultra-large optical band gap, a particularly important field of application of bipolar Ga_2O_3 transparent electrodes is as conducting electrodes for deep ultraviolet light emitting diodes and sensors.

Acknowledgements

We would like to thank NANOVATION (www.nanovation.com) for providing the β-Ga_2O_3/*c*-sapphire epiwafers and G.Bouchez for help with optical transmission measurements. APT acknowledges Agencia Estatal de Investigación (AEI) and Fondo Europeo de Desarrollo Regional (FEDER) under contract ENE2015-74275-JIN and ICN2 authors to the Spanish MINECO through the Severo Ochoa Centers of Excellence Program under Grant SEV-2013-0295.

References

[1] H. von Wenckstern, Group-III Sesquioxides: Growth, Physical Properties and Devices, Adv. Electron. Mater. 93 (2017) 1600350

[2] S. I. Stepanov, V. I. Nikolaev, V. E. Bourgov, A. E. Romanov, Gallium Oxide: properties and applications – a review, Rev. Adv. Mater. Sci. 44 (2016) 63

[3] M. Orita, H. Ohta, M. Hirano, H. Hosono, Deep Ultraviolet Transparent Conductive β-Ga_2O_3 Thin Films, Appl. Phys. Lett. 77 (2000) 4166

[4] M. Higashiwaki, K. Sasaki, T. Kamimura, M. H. Wong, D. Krishnamurthy, A. Kuramata, T. Masui, S. Yamakoshi, Depletion-mode Ga_2O_3 metal-oxide-semiconductor field-effect transistors on β-Ga2O3 (010) substrates and temperature dependence of their device characteristics, Appl. Phys. Lett. 103 (2013) 123511

[5] W.-Y. Kong, G.-A. Wu, K.-Y. Wang, T.-F. Zhang, Y.-F. Zou, D.-D. Wang, L.-B. Luo, Graphene-β-Ga_2O_3 Heterojunction for Highly Sensitive Deep UV Photodetector Application, Adv. Mater. 28 (2016) 10725–10731

[6] P. Feng , J. Y. Zhang , Q. H. Li , T. H. Wang , Individual β-Ga_2O_3 nanowires as solar-blind photodetectors, Appl. Phys. Lett. 88 (2006) 153107

[7] H. H. Tippins, Optical and microwave properties of trivalent chromium in β-Ga_2O_3, Phys. Rev. 137 (1965) A865

[8] T. Minami, T. Shiral, T. Nakatani, T. Miyata, Electroluminescent Devices with Ga_2O_3:Mn Thin-Film Emitting Layer Prepared by Sol-Gel Process, Jpn. J. Appl. Phys. 39 (2000) L524

[9] M. Fleischer, H. Meixner, Selectivity in high-temperature operated semiconductor gas-sensors, Sensors and Actuators B: Chemical 52 (1998) 179

[10] M. A. Mastro, A. Kuramata, J. Calkins, J. Kime, F. Ren, S. J. Pearton, Perspective—Opportunities and Future Directions for Ga_2O_3, ECS Journal of Solid State Science and Technology 6 (2017) P356

[11] M. Higashiwaki, H. Murakami, Y. Kumagai, A. Kuramata, Current status of Ga_2O_3 power devices, Jpn. J. Appl. Phys. 55 (2016) 1202A1

[12] T. P. Chow, I. Omura, M. Higashiwaki, H. Kawarada, V. Pala, Smart Power Devices and ICs Using GaAs and Wide and Extreme Bandgap Semiconductors, IEEE Transactions on Electron Devices 64 (2017) 856

[13] J. Millan, P. Godignon, X. Perpina, A. Perez-Tomas, J. Rebollo, A survey of wide bandgap power semiconductor devices, IEEE Transactions on Power Electronics 29 (2014) 2155

[14] K. Matsuzaki, H. Yanagi, T. Kamiya, H. Hiramatsu, K. Nomura, M. Hirano, H. Yanagi, T. Kamiya, M. Hirano, Growth, structure and carrier transport properties of Ga_2O_3 epitaxial film examined for transparent field-effect transistor, Thin Solid Films 496 (2006) 37

[15] M. Oda, R. Tokuda, H. Kambara, T. Tanikawa, T. Sasaki, T. Hitora, Schottky barrier diodes of corundum-structured gallium oxide showing on-resistance of 0.1 $m\Omega.cm^2$ grown by MIST EPITAXY®, Appl. Phys. Express 9 (2016) 021101

[16] M. Zhong, Z. Wei, X. Meng, F. Wu, J. Li, High-performance single crystalline UV photodetectors of β-Ga_2O_3, J. of Alloys and Compounds 619 (2015) 572

[17] T. Oshima, T. Okuno, N. Arai, N. Suzuki, S. Ohira, S. Fujita, Vertical solar-blind deep-ultraviolet Schottky photodetectors based on β-Ga_2O_3 substrates, Appl. Phys. Express 1 (2008) 011202

[18] Q. He, W. Mu, H. Dong, S. Long, Z. Jia, H. Lu, Q. Liu, M. Tang, X. Tao, M. Liu, Schottky barrier diode based on β-Ga_2O_3 (100) single crystal substrate and its temperature-dependent electrical characteristics, Appl. Phys. Lett. 110 (2017) 093503

[19] FLOSFIA Inc. website, https://www.pntpower.com/flosfia-galo-power/, 2017

[20] Y. Kokubun, S. Kubo, Sh. Nakagomi, All-oxide p–n heterojunction diodes comprising p-type NiO and n-type β-Ga_2O_3, Appl. Phys. Express 9 (2016) 091101

[21] X. C. Guo, N. H. Hao , D.Y. Guo, Z. P. Wu , Y. H. An , X. L. Chu, L. H. Li , P. G. Li, M. Lei, W. H. Tang, β-Ga_2O_3/p-Si heterojunction solar-blind ultraviolet photodetector with enhanced photoelectric responsivity, J. of Alloys and Compounds 660 (2016) 136-140

[22] Y. Qu, Z. Wu, M. Ai, D. Guo, Y. An, H. Yang, L. Li, W. Tang, Enhanced Ga_2O_3/SiC ultraviolet photodetector with graphene top electrodes, J. of Alloys and Compounds 680 (2016) 247-251

[23] Chang Shao-Hui, Chen Zhi-Zhan, Huang Wei, Liu Xue-Chao,Chen Bo-Yuan, Li Zheng-Zheng, Shi Er-Wei, Band alignment of Ga_2O_3/6H-SiC heterojunction, Chin. Phys. B 20 (2011) 116101

[24] B. K. Meyer, A. Polity, D. Reppin, M. Becker, P. Hering, P. J. Klar, Th. Sander, C. Reindl, J. Benz, M. Eickhoff, C. Heiliger, M. Heinemann, J. Blasing, A. Krost, S. Shokovets,C. Müller, C. Ronning, Binary copper oxide semiconductors: From materials towards devices, Phys. Status Solidi B 249 (2012) 1487–1509

[25] K. Ellmer, Past achievements and future challenges in the development of optically transparent electrodes, Nature Phot. 6 (2012) 809

[26] Kelvin H. L. Zhang, Kai Xi, Mark G Blamire, R.G. Egdell, P-type transparent conducting oxides, J. Phys.: Condens. Matter 28 (2016) 383002

[27] H. Sato. T. Minami. S. Takata. T. Yamada, Transparent conducting p-type NiO thin films prepared by magnetron sputtering, Thin Solid Films 236 (1993) 27-31

[28] H. Hiramatsu, K. Ueda, H. Ohta, M. Hirano, M. Kikuchi, H. Yanagi, T. Kamiyae, H. Hosono, Heavy hole doping of epitaxial thin films of a wide gap p-type semiconductor, LaCuOSe, and analysis of the effective mass, Appl. Phys. Lett. 91 (2007) 012104

[29] Z. Wang , P.K. Nayak , J.A. Caraveo-Frescas , Husam N. Alshareef, Recent Developments in p-Type Oxide Semiconductor Materials and Devices, Adv. Mater. 28 (2016) 3831-3892

[30] M. Higashiwaki, K. Sasaki, H. Murakami, Y. Kumagai, A. Koukitu, A. Kuramata, T. Masui S. Yamakoshi, Recent progress in Ga_2O_3 power devices, Semicond. Sci. Technol. 31 (2016) 034001

[31] K. Irmscher, Z. Galazka, M. Pietsch, R. Uecker, R. Fornari, Electrical properties of β-Ga_2O_3 single crystals grown by the Czochralski method, J. Appl. Phys. 110 (2011) 063720

[32] Z. Li Ying, Y. Jin Liang, Z. Yi Jun, L. Ting, D. Xing Wei, First-principles study on electronic structure and optical properties of N-doped P-type β-Ga_2O_3, Sci. China Phys. Mech. Astron.55 (2012) 19-24

[33] C. Tang, J. Sun, N. Lin, Z. Jia, W. Mu, X. Tao, X. Zhao, Electronic structure and optical property of metal-doped Ga_2O_3: a first principles study, RSC Adv. 6 (2016) 78322

[34] H. Raebiger, S. Lany, A. Zunger, Origins of the p-type nature and cation deficiency in Cu_2O and related materials, Phys. Rev. B 76 (2007) 045209

[35] F. H. Teherani, D. J. Rogers, V. E. Sandana, P. Bove, C. Ton-That, L. L. C. Lem, E. Chikoidze, M. Neumann-Spallart, Y. Dumont, T. Huynh, M. R. Phillips, P. Chapon, R. McClintock, M. Razeghi, Investigations on the substrate dependence of the properties in nominally-undoped β-Ga_2O_3 thin films grown by PLD, Proc. of SPIE 10105 (2017) 10105R-1

[36] S.-L. Ou, D.-S. Wuu, Y.-C. Fu, S.-P. Liu, R.-H. Horng, L. Liu, Growth and etching characteristics of gallium oxide thin films by pulsed laser deposition, Mat. Chem. and Phys. 133 (2012) 700-705

[37] A. Goyal, B. S. Yadav, O. P. Thakur, A. K. Kapoor, R. Muralidharan, Effect of annealing on β-Ga_2O_3 film grown by pulsed laser deposition technique, J. of Alloys and Compounds 583 (2014) 214-219

[38] T. Minami, Y. Nishi, T.Miyata, Heterojunction solar cell with 6% efficiency based on an n-type aluminum–gallium–oxide thin film and p-type sodium-doped Cu_2O sheet, Appl. Phys. Express 8 (2015) 022301

[39] M. Orita, H. Hiramatsu, H. Ohta, M. Hirano, H. Hosono, Preparation of highly conductive, deep ultraviolet transparent β-Ga_2O_3 thin film at low deposition temperatures, Thin Solid Films 411 (2002) 134

[40] W. Mi, J. Ma, C. Luan, H. Xiao, Structural and optical properties of β-Ga_2O_3 films deposited on $MgAl_2O_4$ (1 0 0) substrates by metal–organic chemical vapor deposition, J. of Luminescence 146 (2014) 1

[41] H.C. Kang, Heteroepitaxial growth of multidomain Ga_2O_3/sapphire(001) thin films deposited using radio frequency magnetron sputtering, Materials Letters 119 (2014) 123

[42] M. Grundmann, F. Klufel, R. Karsthof, P. Schlupp, F.-L. Schein, D. Splith, C. Yang, S. Bitter, H. von Wenckstern, Oxide bipolar electronics: materials, devices and circuits, J. Phys. D: Appl. Phys. 49 (2016) 213001

[43] E. Chikoidze, H .J. von Bardeleben, K. Akaiwa, E. Shigematsu, K. Kaneko, S. Fujita, Y. Dumont, Electrical, optical, and magnetic properties of Sn doped α-Ga_2O_3 thin films, J. Appl. Phys. 120 (2016) 025109

[44] S. Muller, H. von Wenckstern, D. Splith, F. Schmidt, Marius M. Grundmann, Control of the conductivity of Si-doped β-Ga_2O_3 thin films via growth temperature and pressure, Phys. Status Solidi A 211 (2014) 34

[45] L. Farrell, E. Norton, B. J. O'Dowd, D. Caffrey, I. V. Shvets, K. Fleischer, Spraypyrolysis growth of a high figure of merit, nano-crystalline, p-type transparent conducting material at low temperature, Appl. Phys. Lett. 107 (2015) 031901

[46] J. B. Varley, J. R. Weber, A. Janotti, C. G. Van de Walle, Oxygen vacancies and donor impurities in β-Ga_2O_3, Appl. Phys. Lett. 97 (2010) 142106

[47] L. Binet, D. Gourier, Origin of the Blue Luminescence of β-Ga_2O_3, J. Phys. Chem. Solids 59 (1998) 1241

[48] E. G. Villora, M. Yamaga, T. Inoue, S. Yabasi, Y. Masui, T. Sugawara, T. Fukuda, Optical Spectroscopy Study on β-Ga_2O_3, Jpn. J. Appl. Phys. 41 (2002) L622

[49] S. Kumar, Ch. Tessarek, G. Sarau, S. Christiansen, R. Singh, Self-catalytic growth of beta–Ga_2O_3 nanostructures by chemical vapor deposition, Adv. Eng. Mat. 17 (2015) 709

[50] M. Michling, D. Schmeißer, Resonant Photoemission at the O1s threshold to characterize β-Ga_2O_3 single crystals, IOP Conference Series: Materials Science and Engineering 34 (2012) 012002.

[51] A. Navarro-Quezada, S. Alamé, N. Esser, J. Furthmuller, F. Bechstedt, Z. Galazka, D. Skuridina, P. Vogt, Near valence-band electronic properties of semiconducting β−Ga_2O_3 (100) single crystals, Phys. Rev. B 92 (2015) 195306

[52] P. Richard, T. Sato, S. Souma, K. Nakayama, H. W. Liu, K. Iwaya, T. Hitosugi, H. Aida, H. Ding, T. Takahashi, Observation of momentum space semi-localization in Si-doped β-Ga_2O_3, Appl. Phys. Lett. 101 (2012) 232105

[53] A. Navarro-Quezada, Z. Galazka, S. Alamé, D. Skuridina, P. Vogt, N. Esser, Surface properties of annealed semiconducting β-Ga_2O_3 (100) single crystals for epitaxy, Appl. Surf. Sci. 349 (2015) 368

[54] C. Cocchi, H. Zschiesche, D. Nabok, A. Mogilatenko, M. Albrecht, Z. Galazka, H. Kirmse, C. Draxl, C.T. Koch, Atomic signatures of local environment from core-level spectroscopy in β−Ga_2O_3, Phys. Rev. B 94 (2016) 075147

[55] H. He, R. Orlando, Miguel A. Blanco, R. Pandey, E. Amzallag, I. Baraille, M. Rérat, First-principles study of the structural, electronic, and optical properties of Ga_2O_3 in its monoclinic and hexagonal phases, Phys. Rev. B 74 (2006) 195123

[56] F. Litimein, D. Rached, R. Khenata, H. Baltache, FPLAPW study of the structural, electronic, and optical properties of Ga_2O_3: Monoclinic and hexagonal phases, J. of Alloys and Compounds 488 (2009) 148-156

[57] F.A. Kroger, "The chemistry of imperfect crystals", North-Holland Publishing Company, Amsterdam, 1964, pp.1039

[58] T. Tchelidze, T. Kereselidze, T. Nadareishvili, Perspectives of enhancement of p-type conductivity in ZnO nanowires, Phys. Status Solidi C 12 (2015) 111

[59] M. A. Blanco, M. B. Sahariah, H. Jiang, A. Costales, R. Pandey, Energetics and migration of point defects in Ga_2O_3, Phys. Rev. B 72 (2005) 184103

[60] T. Zacherle, P. C. Schmidt, M. Martin, Ab initio calculations on the defect structure of β-Ga_2O_3, Phys. Rev. B 87 (2013) 235206

[61] T. C. Lovejoy, Renyu Chen, Zheng, E. G. Villora, K. Shimamura, H. Yoshikawa, Y. Yamashita, S. Ueda, K. Kobayashi, S. T. Dunham, F. S. Ohuchi, M. A. Olmstead, Band bending and surface defects in β-Ga_2O_3, Appl. Phys. Lett. 100 (2012) 181602

[62] M. D. Heinemann, J. Berry, G. Teeter, D. Ginley, Oxygen deficiency and Sn doping of amorphous Ga_2O_3, Appl. Phys. Lett. 108 (2016) 022107

[63] D. Segev, S. H. Wei, Structure-derived electronic and optical properties of transparent conducting oxides, Phys. Rev. B 71 (2005) 125129

[64] E. Chikoidze, M. Boshta, M. Gomaa, T. Tchelidze, D. Daraselia, D. Japaridze, A. Shengelaya, Y. Dumont, M. Neumann-Spallart, Control of p-type conduction in Mg doped monophase $CuCrO_2$ thin layers, J. Phys. D: Appl. Phys. 49 (2016) 205107

[65] R. Nagarajan, N. Duan, M.K. Jayaraj, J. Li, K.A. Vanaja, A. Yokochi, A. Draeseke, J. Tate, A.W. Sleight, p-Type conductivity in the delafossite structure, J. Inorg. Mater. 3 (2001) 265-270

[66] A. Kudo, H. Yanagi, H. Hosono, H. Kawazoe, $SrCu_2O_2$: A p-type conductive oxide with wide band gap, Appl. Phys. Lett. 73 (1998) 220

[67] P. Gupta, T. Dutta, S. Mal, J. Narayan, Controlled p-type to n-type conductivity transformation in NiO thin films by ultraviolet-laser irradiation, J. Appl. Phys. 111 (2012) 013706

[68] E. Chikoidze, T. Tchelidze, E. Popova, P. Maso, N. Ponjavidze, N. Keller, Y. Dumont, Conductivity type inversion in wide band gap antiferromagnetic $FeTiO_3$, Appl. Phys. Lett. 102 (2013) 122112

[69] R. Pérez, D. Tournier, A. Pérez-Tomás, P. Godignon, N. Mestres, J. Millán, Planar edge termination design and technology considerations for 1.7-kV 4H-SiC PiN diodes, IEEE Transactions on Electron Devices 52 (2005) 2309